Investigation of the $\Delta I = 1/2$ Rule and Test of CP Symmetry through the Measurement of Decay Asymmetry Parameters in Ξ^- Decays

M. Ablikim *et al.*[*]
(BESIII Collaboration)

(Received 26 September 2023; accepted 1 February 2024; published 6 March 2024)

Using $(10087 \pm 44) \times 10^6$ J/ψ events collected with the BESIII detector, numerous Ξ^- and Λ decay asymmetry parameters are simultaneously determined from the process $J/\psi \to \Xi^-\bar{\Xi}^+ \to \Lambda(p\pi^-)\pi^-\bar{\Lambda}(\bar{n}\pi^0)\pi^+$ and its charge-conjugate channel. The precisions of $\alpha_{\Lambda 0}$ for $\Lambda \to n\pi^0$ and $\bar{\alpha}_{\Lambda 0}$ for $\bar{\Lambda} \to \bar{n}\pi^0$ compared to world averages are improved by factors of 4 and 1.7, respectively. The ratio of decay asymmetry parameters of $\Lambda \to n\pi^0$ to that of $\Lambda \to p\pi^-$, $\langle\alpha_{\Lambda 0}\rangle/\langle\alpha_{\Lambda -}\rangle$, is determined to be $0.873 \pm 0.012^{+0.011}_{-0.010}$, where the first and the second uncertainties are statistical and systematic, respectively. The ratio is smaller than unity more than 5σ, which signifies the existence of the $\Delta I = 3/2$ transition in Λ for the first time. Besides, we test for CP symmetry in $\Xi^- \to \Lambda\pi^-$ and in $\Lambda \to n\pi^0$ with the best precision to date.

DOI: 10.1103/PhysRevLett.132.101801

The noninvariance of fundamental interactions under the combination of charge-conjugation (C) and parity (P) transformations is a necessary condition for baryogenesis [1], a process that dynamically generates the matter-antimatter asymmetry in the Universe. Although the standard model (SM) accommodates CP violation with the Kobayashi-Maskawa phase [2,3], it can only explain a matter-antimatter asymmetry that is at least 10 orders of magnitude smaller than the observed value [4]. Additional sources of CP violation beyond the SM are expected to exist, and the weak hadronic transitions of hyperons are another place to search for such sources of CP violation [5,6].

When two or more transition amplitudes interfere with each other, relative weak- and strong-phase contributions exist between them. For $K \to \pi\pi$ [7,8], the CP violating weak phase comes from the interference between S-wave isospin $I = 0$ (A_0) and isospin $I = 2$ (A_2) amplitudes, which correspond to $\Delta I = 1/2$ and $\Delta I = 3/2$ transitions, respectively [9]. The unforeseen large discrepancy between the real parts of the two isospin amplitudes, $\mathrm{Re}(A_0)/\mathrm{Re}(A_2) = 22.45 \pm 0.06$, known as the $\Delta I = 1/2$ rule [10,11], is a long-standing puzzle. Various theoretical models have been proposed to explain this large ratio, but the dual QCD approach [12] and lattice QCD calculation [13] can only partially explain it. A comprehensive understanding of this rule is desirable.

The $\Delta I = 1/2$ rule is also applicable in the decays of spin $1/2$ hyperons [14,15], which can be described in terms of its decay asymmetry parameters, α_{Y} and ϕ_{Y} [16]. The ratio of decay asymmetry parameters for the two isospin decay modes $\Lambda \to n\pi^0$ and $\Lambda \to p\pi^-$, $\alpha_{\Lambda 0}/\alpha_{\Lambda -}$, is a sensitive probe to determine the contribution of $\Delta I = 3/2$ transitions. In their absence, the ratio $\alpha_{\Lambda 0}/\alpha_{\Lambda -}$ is predicted to be unity [15]. A recent BESIII result suggests that this might not be the case [17]. Further studies of the isospin amplitude in hyperon decays are required to rigorously test the $\Delta I = 1/2$ rule.

Moreover, contrary to kaon decays, CP violation in hyperon decays could arise from the interference between parity-conserving (P-wave) and parity-violating (S-wave) amplitudes with a CP-odd weak phase. The decay asymmetry parameters of hyperon are CP-odd and assuming CP conservation $\alpha_{\mathrm{Y}} = -\bar{\alpha}_{\mathrm{Y}}$ and $\phi_{\mathrm{Y}} = -\bar{\phi}_{\mathrm{Y}}$, where $\bar{\alpha}_{\mathrm{Y}}$ and $\bar{\phi}_{\mathrm{Y}}$ are decay asymmetry parameters for antihyperon $\bar{Y}$ [6]. CP symmetry, which is broken in the presence of non-negligible weak-phase contributions, is gauged by the CP observables A_{CP} and $\Delta\phi_{CP}$ [18]:

$$A_{CP}^{\mathrm{Y}} = \frac{\alpha_{\mathrm{Y}} + \bar{\alpha}_{\mathrm{Y}}}{\alpha_{\mathrm{Y}} - \bar{\alpha}_{\mathrm{Y}}} = -\tan(\delta_P - \delta_S)\tan(\xi_P - \xi_S), \quad (1)$$

$$\Delta\phi_{CP}^{\mathrm{Y}} = \frac{\phi_{\mathrm{Y}} + \bar{\phi}_{\mathrm{Y}}}{2} = \frac{\langle\alpha\rangle}{\sqrt{1 - \langle\alpha\rangle^2}}\cos\langle\phi\rangle\tan(\xi_P - \xi_S), \quad (2)$$

where $\langle\alpha\rangle = (\alpha_{\mathrm{Y}} - \bar{\alpha}_{\mathrm{Y}})/2$, $\langle\phi\rangle = (\phi_{\mathrm{Y}} - \bar{\phi}_{\mathrm{Y}})/2$, $\delta_P - \delta_S$ denotes the strong-phase difference of the final-state interaction, and $\xi_P - \xi_S$ denotes the weak-phase difference. Experimentally, the weak-phase difference has been directly determined to be $(1.2 \pm 3.4 \pm 0.8) \times 10^{-2}$ rad [18] for the

[*]Full author list given at the end of the Letter.

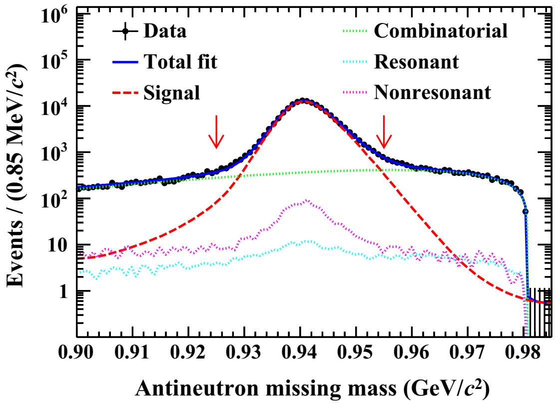

FIG. 1. Distribution of antineutron missing mass. The data are shown as black data points with error bars. The blue solid curve represents the total fit result, and the red dashed line denotes the signal shape. The dotted lines in green, light blue, and magenta denote the combinatorial, resonant, and nonresonant background contributions, respectively. The red arrows indicate the signal region.

decay $\Xi^- \to \Lambda\pi^-$ using entangled Ξ^- and $\bar{\Xi}^+$ produced at BESIII.

In this Letter, the process $J/\psi \to \Xi^-\bar{\Xi}^+ \to \Lambda(p\pi^-)\pi^-\bar{\Lambda}(\bar{n}\pi^0)\pi^+$ is studied with $(10087 \pm 44) \times 10^6$ J/ψ events [19] collected by the BESIII detector. Benefiting from the transversely polarized hyperons and the spin correlation between hyperon and antihyperons, various decay properties of Ξ^- and Λ are determined by an extended formalism that completely describes the angular distributions of the production and decay processes [20].

The design and performance of the BESIII detector are described in Refs. [21,22]. The corresponding simulation, analysis framework, and software are presented in Refs. [23–25]. Simulated Monte Carlo (MC) samples are produced with Geant4-based [26] MC software, which models the experimental conditions, including the electron-positron collision, the decays of the particles, and the response of the detector. A sample of simulated events of generic J/ψ decays, corresponding to the luminosity of data, is used to study the potential background reactions. To eliminate experimenter bias, the central values were blinded by using the hidden answer technique [27] until all selections, fits, and uncertainty evaluations were finalized. Simulated signal and background samples are used to verify the analysis approaches and to study the systematic effects. Unless otherwise indicated, the charge-conjugate channel is implied throughout the text.

Four charged tracks are required in the multilayer drift chamber within the range $|\cos\theta| < 0.93$, where θ is the polar angle with respect to the z axis, which is the symmetry axis of the multilayer drift chamber. Because of the nonoverlapping momentum ranges of the proton and pions, a positively charged track with momentum greater than 0.32 GeV/c is assigned to be a proton, while a positively and two negatively charged tracks with momentum less than 0.30 GeV/c are assigned to be pions. The probability of misidentifying a proton for a π^+ is negligible. The sequential decay $\Xi^- \to \Lambda\pi^- \to p\pi^-\pi^-$ is reconstructed by a vertex fit [18,28], which takes into account the flight paths of the hyperons. The combination with the smallest $(M_{p\pi^-\pi^-} - m_{\Xi^-})^2 + (M_{p\pi^-} - m_\Lambda)^2$ is retained, where $M_{p\pi^-\pi^-(p\pi^-)}$ denotes the invariant mass of $p\pi^-\pi^-$ $(p\pi^-)$ and $m_{\Xi^-(\Lambda)}$ refers to the nominal mass of Ξ^- (Λ) [29]. The probability of a π^- from the Λ and Ξ^- decays being wrongly assigned is found to be 0.1%, which is negligible. The candidate events are required to satisfy $|M_{p\pi^-} - m_\Lambda| < 11\ \mathrm{MeV/c^2}$ and $|M_{p\pi^-\pi^-} - m_{\Xi^-}| < 11\ \mathrm{MeV/c^2}$. The decay lengths of the Ξ^- and Λ are calculated in the vertex fit and required to be positive. To improve the resolution and minimize the discrepancy between data and MC simulation, the polar angle θ_{Ξ^-} of the reconstructed Ξ^- in the e^+e^- center-of-mass frame is required to satisfy $|\cos\theta_{\Xi^-}| < 0.84$.

At least two photon candidates in the electromagnetic calorimeter (EMC) are required. A photon candidate should have energy greater than 25 MeV in the barrel region ($|\cos\theta| < 0.8$) or 50 MeV in the end-cap region ($0.86 < |\cos\theta| < 0.92$). For antiprotons, which may annihilate in the detector, photon candidates must be separated from charged tracks with an opening angle greater than 20°, while for other tracks the angle must be greater than 10°. To suppress electronic noise and showers unrelated to the event, photon candidates are required to have the EMC time difference from the event start time within [0, 700] ns. To veto the showers from antineutron interactions in the EMC, the photon candidates should be separated from the direction of the $\Xi^-\pi^+$ recoiling system with an opening angle greater than 15°. A boosted decision tree classifier [30] is constructed based on the shower shape variables to discriminate a signal photon from a noise shower. The shower shape variables include the deposited energy, number of hits, second and Zernike moments, and deposition shape [31]. The signal efficiency of the boosted decision tree is 90%, and 55% of the background is rejected. The π^0 candidates are reconstructed from a pair of photons by constraining their invariant mass to the π^0 nominal mass, and the corresponding χ^2_{1C} is required to be less than 25. Because of combinatorial effects, it is possible to have more than one unique π^0 candidate in a single event.

A kinematic fit under the hypothesis of $J/\psi \to \Xi^-\pi^+\bar{n}\gamma\gamma$ is performed imposing energy-momentum conservation and constraining the invariant masses of $\gamma\gamma$ and $\gamma\gamma\bar{n}$ to the nominal masses of π^0 and $\bar{\Lambda}$, respectively. The kinematics of the Ξ^- are obtained from the above vertex fit. The antineutron is treated as a missing particle with unknown mass. The fit is performed for each π^0 candidate. If there is more than one π^0 candidate, the candidate with the smallest χ^2 is retained, and $\chi^2 < 200$ is required. The invariant mass of $\bar{n}\gamma\gamma\pi^+$ is required to satisfy

$|M_{\bar{n}\gamma\gamma\pi^+} - m_{\bar{\Xi}^+}| < 11\ \mathrm{MeV}/c^2$. Since all other final state particles are detected, the kinematic fit allows for the reconstruction of the four momentum of antineutron. The signal is identified by the antineutron's missing mass, as shown in Fig. 1 with a prominent signal peak in the antineutron vicinity and a low level background.

Detailed studies are performed with MC simulation and data in the Ξ^- and $\bar{\Xi}^+$ sideband regions to evaluate the potential backgrounds. The dominant background, referred to as combinatorial background, is from signal events with misreconstructed π^0 candidates, which do not peak in the antineutron missing mass distribution. The remaining background sources are classified into two categories [32]: resonant background that contains $\Xi^-\bar{\Xi}^+$ intermediate states, such as, $J/\psi \to \gamma\eta_c \to \gamma\Xi^-\bar{\Xi}^+ \to \gamma\Lambda(\to p\pi^-)\pi^-\bar{\Lambda}(\bar{n}\pi^0)\pi^+$ and $J/\psi \to \Xi^-\bar{\Xi}^+ \to \Lambda(\to p\pi^-)\pi^-\bar{\Lambda}(\bar{p}\pi^+)\pi^+$; nonresonant background without $\Xi^-\bar{\Xi}^+$ intermediate states. The decay processes of resonant backgrounds are well understood, and the corresponding contributions are evaluated by MC simulation, which are generated according to the helicity amplitudes and weighted according to the branching fractions [29]. MC simulation shows that the distributions of $M_{p\pi^-\pi^-}$ and $M_{\bar{n}\gamma\gamma\pi^+}$ of nonresonant background are almost flat. Therefore, the corresponding contribution can be evaluated from the Ξ^- and $\bar{\Xi}^+$ sideband regions.

Signal yields are obtained from an unbinned maximum likelihood fit of the missing mass distribution. In the fit shown in Fig. 1, the signal is described by an MC-simulated shape convolved by a Gaussian function accounting for the resolution difference between data and MC simulation. The combinatorial background is described by the signal MC sample, and it is parametrized by a product of an ARGUS function [33] and a cubic function. Fixing both the magnitude and shape, the resonant and nonresonant backgrounds are described with the MC simulation and data events in the sideband region, respectively. The normalization of the background and the definition of the sideband region are shown in Sec. 2 of the Supplemental Material [34]. The fit yields 143973 ± 414 signal events and a purity of 91.2% in the mass range $[0.925, 0.955]\ \mathrm{GeV}/c^2$. The same procedure is performed for the charge-conjugate process and results in $123\,208 \pm 382$ signal events and a purity of 91.0%.

The joint angular amplitude of the full decay chain can be written in a modular form as

$$\mathcal{W}(\xi;\omega) = \sum_{\mu,\nu=0}^{3} C_{\mu\nu} \sum_{\mu',\nu'=0}^{3} a^{\Xi}_{\mu\mu'} a^{\bar{\Xi}}_{\nu\nu'} a^{\Lambda}_{\mu'0} a^{\bar{\Lambda}}_{\nu'0}. \quad (3)$$

Here, $C_{\mu\nu}$ is a 4×4 real-valued spin density matrix describing the spin configuration of the entangled $\Xi^-\bar{\Xi}^+$ pair, $a^{\mathrm{Y}}_{\mu\nu}$ is also a 4×4 real-valued matrix representing the propagation of the spin density matrix in the decays of a spin 1/2 hyperon into a spin 1/2 baryon and a pseudoscalar, $\mathrm{Y} \to \mathrm{B}\pi$. Therefore, the distribution of the nine helicity angles $\xi = (\theta_\Xi, \theta_\Lambda, \phi_\Lambda, \theta_{\bar{\Lambda}}, \phi_{\bar{\Lambda}}, \theta_p, \phi_p, \theta_{\bar{n}}, \phi_{\bar{n}})$ is determined by eight global parameters $\omega = (\alpha_{J/\psi}, \Delta\Phi_{J/\psi}, \alpha_\Xi, \phi_\Xi, \bar{\alpha}_\Xi, \bar{\phi}_\Xi, \alpha_{\Lambda-}, \bar{\alpha}_{\Lambda0})$. In this analysis, $\mathrm{Y} \to \mathrm{B}\pi$ stands for $\Xi^- \to \Lambda\pi^-$, $\Lambda \to p\pi^-$, and $\bar{\Lambda} \to \bar{n}\pi^0$. The distribution of the helicity angle θ_p in the Λ rest frame is written as

$$\frac{\mathrm{d}N}{\mathrm{d}\cos\theta_p} \propto 1 + \alpha_{\Lambda-}\alpha_\Xi \cos\theta_p \quad (4)$$

by integrating over the remaining eight helicity angles. The formalism of the full angular distribution and the definition of the reference system are discussed in detail in Ref. [18].

A simultaneous fit on the joint angular distribution is carried out with the production parameters, $\alpha_{J/\psi}$ and $\Delta\Phi_{J/\psi}$, and decay asymmetry parameters of Ξ^- shared between the two charge-conjugate channels. For each channel, the probability distribution function of the eight unknown parameters ω can be defined in terms of the helicity angles ξ

$$\mathcal{P}(\xi;\omega) = \mathcal{W}(\xi;\omega)\varepsilon(\xi)/\mathcal{N}(\omega), \quad (5)$$

where the normalization factor $\mathcal{N}(\omega)$ is calculated with $\mathcal{N}(\omega) = (1/M)\sum_{j=1}^{M}[\mathcal{W}(\xi_j;\omega)/\mathcal{W}(\xi_j;\omega_{\mathrm{gen}})]$ by a signal MC sample generated with parameters ω_{gen}. The sum runs over all events in the generated sample M, which is chosen to be 30 times the yield obtained in data after the full selection. The log-likelihood function for N observed events is

$$\mathcal{S} = -\mathcal{G}\left(\sum_{i=1}^{N} \ln\mathcal{P}(\xi_i;\omega) - \sum_j w_j \sum_i^{N_j^{\mathrm{bkg}}} \ln\mathcal{P}(\xi_i;\omega)\right), \quad (6)$$

where the second term in brackets with j from one to three represents the three different sources of background remaining in the final event sample. Their contributions are evaluated with the corresponding MC samples or data events in the sideband region and their associated weight factors w_j. The global factor, $\mathcal{G} = (N - \sum_j N_j^{\mathrm{bkg}} \times w_j)/(N + \sum_j N_j^{\mathrm{bkg}} \times w_j^2)$, corrects for the statistical uncertainties in the weighted likelihood fit [35].

The $\mathcal{S}$ function is minimized using Minuit2 [36] to determine the production and decay asymmetry parameters ω. The results from the fit, as shown in Table I, are consistent with previous measurements, but with improved precision. In particular, $\alpha_{\Lambda0}$ is almost the same in magnitude and opposite in sign as $\bar{\alpha}_{\Lambda0}$, and its precision is improved by a factor of 4 over previous measurements.

If CP is conserved, the product of the decay asymmetry parameters $\alpha_{\Lambda-}\alpha_\Xi$ and $\alpha_{\Lambda+}\bar{\alpha}_\Xi$ should be equal to each

TABLE I. The production and decay asymmetry parameters, the weak- and strong-phase differences from Ξ^- decay, the tests of CP symmetry, and the ratios of decay asymmetry parameters, $\alpha_{\Lambda 0}/\alpha_{\Lambda -}$ and $\bar{\alpha}_{\Lambda 0}/\alpha_{\Lambda +}$. The first and second uncertainties are statistical and systematic, respectively.

Parameters	This work	Previous result
$\alpha_{J/\psi}$	$0.611 \pm 0.007^{+0.013}_{-0.007}$	$0.586 \pm 0.012 \pm 0.010$ [18]
$\Delta\Phi_{J/\psi}$ (rad)	$1.30 \pm 0.03^{+0.02}_{-0.03}$	$1.213 \pm 0.046 \pm 0.016$ [18]
α_Ξ	$-0.367 \pm 0.004^{+0.003}_{-0.004}$	$-0.376 \pm 0.007 \pm 0.003$ [18]
ϕ_Ξ (rad)	$-0.016 \pm 0.012^{+0.004}_{-0.008}$	$0.011 \pm 0.019 \pm 0.009$ [18]
$\bar{\alpha}_\Xi$	$0.374 \pm 0.004^{+0.003}_{-0.004}$	$0.371 \pm 0.007 \pm 0.002$ [18]
$\bar{\phi}_\Xi$ (rad)	$0.010 \pm 0.012^{+0.003}_{-0.013}$	$-0.021 \pm 0.019 \pm 0.007$ [18]
$\alpha_{\Lambda -}$	$0.764 \pm 0.008^{+0.005}_{-0.006}$	$0.7519 \pm 0.0036 \pm 0.0024$ [37]
$\alpha_{\Lambda +}$	$-0.774 \pm 0.009^{+0.005}_{-0.005}$	$-0.7559 \pm 0.0036 \pm 0.0030$ [37]
$\alpha_{\Lambda 0}$	$0.670 \pm 0.009^{+0.009}_{-0.008}$	0.75 ± 0.05 [29]
$\bar{\alpha}_{\Lambda 0}$	$-0.668 \pm 0.008^{+0.006}_{-0.008}$	$-0.692 \pm 0.016 \pm 0.006$ [17]
$\delta_P - \delta_S$ (rad)	$0.033 \pm 0.020^{+0.008}_{-0.012}$	$-0.040 \pm 0.033 \pm 0.017$ [18]
$\xi_P - \xi_S$ (rad)	$0.007 \pm 0.020^{+0.018}_{-0.005}$	$0.012 \pm 0.034 \pm 0.008$ [18]
A^Ξ_{CP}	$-0.009 \pm 0.008^{+0.007}_{-0.002}$	$0.006 \pm 0.013 \pm 0.006$ [18]
$\Delta\phi^\Xi_{CP}$ (rad)	$-0.003 \pm 0.008^{+0.003}_{-0.007}$	$-0.005 \pm 0.014 \pm 0.003$ [18]
A^-_{CP}	$-0.007 \pm 0.008^{+0.002}_{-0.003}$	$-0.0025 \pm 0.0046 \pm 0.0012$ [37]
A^0_{CP}	$0.001 \pm 0.009^{+0.005}_{-0.007}$	...
A^Λ_{CP}	$-0.004 \pm 0.007^{+0.003}_{-0.004}$	...
$\alpha_{\Lambda 0}/\alpha_{\Lambda -}$	$0.877 \pm 0.015^{+0.014}_{-0.010}$	1.01 ± 0.07 [29]
$\bar{\alpha}_{\Lambda 0}/\alpha_{\Lambda +}$	$0.863 \pm 0.014^{+0.012}_{-0.008}$	$0.913 \pm 0.028 \pm 0.012$ [17]

other, and the ratios of helicity angular distributions for different nucleons in the final states, $R(\cos\theta_p, \cos\theta_{\bar{p}}) = (1+\alpha_{\Lambda -}\alpha_\Xi\cos\theta_p)/(1+\alpha_{\Lambda +}\bar{\alpha}_\Xi\cos\theta_{\bar{p}})$ and $R(\cos\theta_n, \cos\theta_{\bar{n}}) = (1+\alpha_{\Lambda 0}\alpha_\Xi\cos\theta_n)/(1+\bar{\alpha}_{\Lambda 0}\bar{\alpha}_\Xi\cos\theta_{\bar{n}})$, are flat and equal to unity. In a similar way, if there is no $\Delta I = 3/2$ transition in Λ decay, $\alpha_{\Lambda -}$ should be equal to $\alpha_{\Lambda 0}$ and the ratios, $R(\cos\theta_n, \cos\theta_p) = (1+\alpha_{\Lambda 0}\alpha_\Xi\cos\theta_n)/(1+\alpha_{\Lambda -}\alpha_\Xi\cos\theta_p)$ and $R(\cos\theta_{\bar{n}}, \cos\theta_{\bar{p}}) = (1+\bar{\alpha}_{\Lambda 0}\bar{\alpha}_\Xi\cos\theta_{\bar{n}})/(1+\alpha_{\Lambda +}\bar{\alpha}_\Xi\cos\theta_{\bar{p}})$, are also flat and equal to unity. The accuracy of the CP symmetry and the $\Delta I = 1/2$ rule tests can be improved by using the isospin average for R_1, $R_1 = (1+\alpha_\Lambda\alpha_\Xi\cos\theta)/(1+\bar{\alpha}_\Lambda\bar{\alpha}_\Xi\cos\theta)$, where $\cos\theta$ stands for the helicity angle of nucleon, α_Λ is defined as $(2\alpha_{\Lambda -}+\alpha_{\Lambda 0})/3$, and the average of the decay symmetry parameters of hyperon and antihyperon for R_2, $R_2 = (1+\langle\alpha_{\Lambda 0}\rangle\langle\alpha_\Xi\rangle\cos\theta)/(1+\langle\alpha_{\Lambda -}\rangle\langle\alpha_\Xi\rangle\cos\theta)$.

To illustrate the tests of CP symmetry and the $\Delta I = 1/2$ rule, four ratios of the helicity angular distributions for different nucleons in the final states are shown in Fig. 2 by dots with error bars. R_1 and R_2 with parameters from Table I are also presented in Fig. 2. The ratios obtained by fitting the events in bins of $\cos\theta$ are in good agreement with the global curves obtained for R_1 and R_2. The nearly flat distribution of R_1 is consistent with CP conservation. The sloping distribution of R_2 indicates the existence of the contribution of $\Delta I = 3/2$ transition in Λ decay.

The systematic uncertainties are split into different categories: reconstruction and event selection of the signal candidates, the uncertainties related to the background contributions, and the effects which arise from the final fit procedure. The uncertainty of the π^0 reconstruction is investigated by studying the decay $J/\psi \to \Sigma^+(p\pi^0)\pi^-\bar{\Lambda}(\bar{p}\pi^+)$ + c.c. as it has a similar final state topology and decay length as the signal. The systematic uncertainty from $\pi^\pm$ reconstruction is investigated by using a control sample of $J/\psi \to \Xi^-\bar{\Xi}^+ \to \Lambda(p\pi^-)\pi^-\bar{\Lambda}(\bar{p}\pi^+)\pi^+$ + c.c. The systematic uncertainties due to different resolutions in data and simulation are studied by varying selection criteria (the decay points and invariant masses of Λ and Ξ^-, the polar angle of Ξ^-, the missing mass and the χ^2 of the kinematic fit) around their nominal values and repeating the fit. The uncertainty due to the combinatorial background is determined by both smearing the parameters of model and varying its yield from the fit to the missing mass distribution by $\pm 1\sigma$. The uncertainties associated with the resonant backgrounds, which are propagated from the uncertainties in branching fractions, number of J/ψ events, and MC sample statistics, are also evaluated by varying the background yield by $\pm 1\sigma$. In the case of nonresonant background, the fit is repeated without this background component, and the deviation from the nominal fit is taken as the systematic uncertainty. To estimate the systematic uncertainty of the fit procedure,

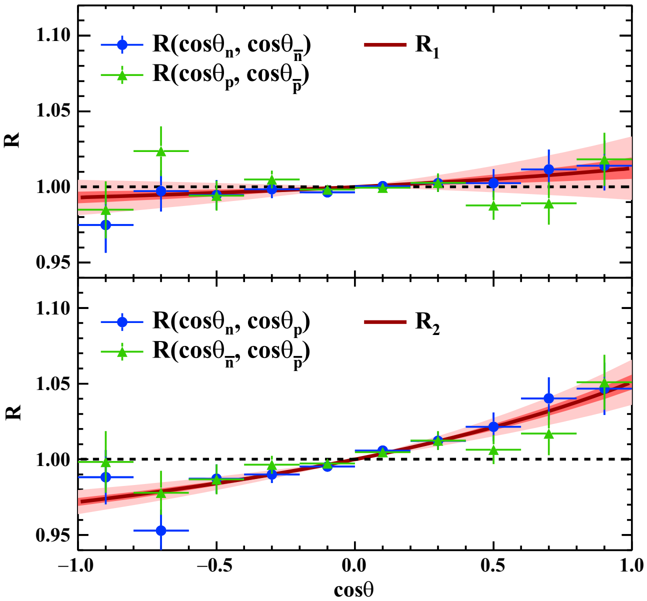

FIG. 2. The ratios of helicity angular distributions for different nucleons in the final states, $R(\cos\theta_p, \cos\theta_{\bar{p}})$ and $R(\cos\theta_n, \cos\theta_{\bar{n}})$ (top) as well as $R(\cos\theta_n, \cos\theta_p)$ and $R(\cos\theta_{\bar{n}}, \cos\theta_{\bar{p}})$ (bottom) versus $\cos\theta$. The dots with errors are determined by independent fits for each $\cos\theta$ bin of the corresponding nucleons. The solid curves in red with 1σ (red) and 3σ (pink) statistical uncertainty bands show the results of the simultaneous fit. The dashed curves in black show the CP-conserving and no $\Delta I = 3/2$ transition expectations.

1000 sets of toy MC samples are generated with the parameters from Table I. Each set is fitted to obtain the distribution of the output parameters. The average values of the difference between the input and output parameters and statistical errors of the average differences are regarded as systematic uncertainties. More details can be found in the Supplemental Material [34].

In summary, the decay asymmetry parameters listed in Table I are simultaneously determined from the process $J/\psi \to \Xi^-\bar{\Xi}^+ \to \Lambda(p\pi^-)\pi^-\bar{\Lambda}(\bar{n}\pi^0)\pi^+$ and its charge-conjugate channel with $(10087 \pm 44) \times 10^6$ J/ψ events collected by the BESIII detector. Using Eqs. (1) and (2), the CP observables A_{CP}^{Ξ} and $\Delta\phi_{CP}^{\Xi}$ for Ξ^- decay, as well as $A_{CP}^- = (\alpha_{\Lambda-} + \alpha_{\Lambda+})/(\alpha_{\Lambda-} - \alpha_{\Lambda+})$ and $A_{CP}^0 = (\alpha_{\Lambda 0} + \bar{\alpha}_{\Lambda 0})/(\alpha_{\Lambda 0} - \bar{\alpha}_{\Lambda 0})$ of the charged and neutral Λ decays, are obtained from the corresponding decay asymmetry parameters and correlations. A_{CP}^{Ξ} and $\Delta\phi_{CP}^{\Xi}$ are measured with world-leading precision, and A_{CP}^0 is measured for the first time. The correlations $\rho(\alpha_{\Lambda-}, \alpha_{\Lambda+})$ and $\rho(\alpha_{\Lambda 0}, \bar{\alpha}_{\Lambda 0})$ measured from two charge-conjugate channels are negligible. The precise CP symmetry test of the Λ decay is conducted with its isospin averages, $A_{CP}^{\Lambda} = (2A_{CP}^- + A_{CP}^0)/3$, which improves the sensitivity of the CP symmetry test by 20% compared to the individual tests for each isospin decay mode. The strong-phase and weak-phase differences of $\Xi^- \to \Lambda\pi^-$, derived from Eqs. (1) and (2), are both consistent with previous BESIII results [18]. The strong-phase difference is also in agreement with the HyperCP measurement [38]. The CP symmetry is conserved in the decay of Ξ^- and Λ within the current precision. The theoretical predictions within the SM [39,40] are $0.5 \times 10^{-5} \leqslant (A_{CP}^{\Xi})_{\rm SM} \leqslant 6 \times 10^{-5}$, $-3.8 \times 10^{-4} \leqslant (\xi_P - \xi_S)_{\rm SM} \leqslant -0.3 \times 10^{-4}$ and $-3 \times 10^{-5} \leqslant (A_{CP}^{\Lambda})_{\rm SM} \leqslant 3 \times 10^{-5}$.

The ratios of $\alpha_{\Lambda 0}/\alpha_{\Lambda-}$ and $\bar{\alpha}_{\Lambda 0}/\alpha_{\Lambda+}$ deviate from unity by more than 5 standard deviations, which signifies the existence of the $\Delta I = 3/2$ transition in both Λ and $\bar{\Lambda}$ decays for the first time. Using the averages of the ratio $\langle\alpha_{\Lambda 0}\rangle/\langle\alpha_{\Lambda-}\rangle = 0.870 \pm 0.012^{+0.011}_{-0.010}$ with combinations of the decay rates $\Gamma(\Lambda \to p\pi^-)$, $\Gamma(\Lambda \to n\pi^0)$ [29] and the N-π scattering phase shift [41], the ratio of $\Delta I = 1/2$ to $\Delta I = 3/2$ transitions in S wave is determined to be $S_1/S_3 = 28.4 \pm 1.3^{+1.1}_{-1.0} \pm 3.9$, while in P wave $P_1/P_3 = -13.0 \pm 1.4^{+1.1}_{-1.2} \pm 0.7$ according to Ref. [5], where the first uncertainties are statistical, the second systematic, and the third from the input parameters. The ratio in S wave is consistent with $\mathrm{Re}(A_0)/\mathrm{Re}(A_2)$ in $K \to \pi\pi$ within the uncertainty, while the ratio in P wave is measured for the first time and found different from that in S wave. This measurement provides a constraint for lattice QCD [13] and dual QCD [12] approach to understand the $\Delta I = 1/2$ rule.

The authors thank Professor X. G. He and Professor X. Feng for helpful discussions. The BESIII Collaboration thanks the staff of BEPCII and the IHEP computing center and the supercomputing center of the University of Science and Technology of China (USTC) for their strong support. This work is supported in part by National Key R&D Program of China under Contracts No. 2020YFA0406400, 2020YFA0406300, No. 2023YFA1609400; National Natural Science Foundation of China (NSFC) under Contracts No. 11635010, No. 11735014, No. 11835012, No. 11935015, No. 11935016, No. 11935018, No. 11961141012, No. 12022510, No. 12025502, No. 12035009, No. 12035013, No. 2061131003, No. 12192260, No. 12192261, No. 12192262, No. 12192263, No. 12192264, No. 12192265, No. 12221005, No. 12225509, No. 12235017, No. 12122509, No. 12105276, No. 11625523; the Chinese Academy of Sciences (CAS) Large-Scale Scientific Facility Program; the CAS Center for Excellence in Particle Physics (CCEPP); Joint Large-Scale Scientific Facility Funds of the NSFC and CAS under Contracts No. U1832207, No. U2032111, No. U1732263, No. U1832103; CAS Key Research Program of Frontier Sciences under Contracts No. QYZDJ-SSW-SLH003, No. QYZDJ-SSW-SLH040; 100 Talents Program of CAS; The Institute of Nuclear and Particle Physics (INPAC) and Shanghai Key Laboratory for Particle Physics and Cosmology; European Union's Horizon 2020 research and innovation programme under Marie Sklodowska-Curie grant agreement under Contract

No. 894790; German Research Foundation DFG under Contract No. 455635585, Collaborative Research Center CRC 1044, FOR5327, GRK 2149; Istituto Nazionale di Fisica Nucleare, Italy; Ministry of Development of Turkey under Contract No. DPT2006K-120470; National Research Foundation of Korea under Contract No. NRF-2022R1A2C1092335; National Science and Technology fund of Mongolia; National Science Research and Innovation Fund (NSRF) via the Program Management Unit for Human Resources and Institutional Development, Research and Innovation of Thailand under Contract No. B16F640076; Polish National Science Centre under Contract No. 2019/35/O/ST2/02907; The Knut and Alice Wallenberg Foundation, Sweden, the Swedish Research Council, the Swedish Foundation for International Cooperation in Research and Higher Education (STINT); U.S. Department of Energy under Contract No. DE-FG02-05ER41374; Olle Engkvist Foundation under Contract No. 200-0605 and Lundström-Åman Foundation. CAS Youth Team Program under Contract No. YSBR-101.

[1] A. D. Sakharov, Pis'ma Zh. Eksp. Teor. Fiz. **5**, 32 (1967).
[2] N. Cabibbo, Phys. Rev. Lett. **10**, 531 (1963).
[3] M. Kobayashi and T. Maskawa, Prog. Theor. Phys. **49**, 652 (1973).
[4] S. M. Barr, G. Segre, and H. A. Weldon, Phys. Rev. D **20**, 2494 (1979).
[5] N. Salone, P. Adlarson, V. Batozskaya, A. Kupsc, S. Leupold, and J. Tandean, Phys. Rev. D **105**, 116022 (2022).
[6] J. F. Donoghue, X.-G. He, and S. Pakvasa, Phys. Rev. D **34**, 833 (1986).
[7] A. Alavi-Harati *et al.* (KTeV Collaboration), Phys. Rev. Lett. **83**, 22 (1999).
[8] V. Fanti *et al.* (NA48 Collaboration), Phys. Lett. B **465**, 335 (1999).
[9] V. Cirigliano, G. Ecker, H. Neufeld, A. Pich, and J. Portoles, Rev. Mod. Phys. **84**, 399 (2012).
[10] Y. S. Amhis *et al.* (HFLAV Collaboration), Phys. Rev. D **107**, 052008 (2023).
[11] C. A. Manzari, A. M. Coutinho, and A. Crivellin, Proc. Sci. LHCP2020 (**2021**) 242.
[12] A. J. Buras, J.-M. Gérard, and W. A. Bardeen, Eur. Phys. J. C **74**, 2871 (2014).
[13] R. Abbott *et al.* (RBC and UKQCD Collaborations), Phys. Rev. D **102**, 054509 (2020).
[14] O. E. Overseth and S. Pakvasa, Phys. Rev. **184**, 1663 (1969).
[15] S. Olsen, L. Pondrom, R. Handler, P. Limon, J. A. Smith, and O. E. Overseth, Phys. Rev. Lett. **24**, 843 (1970).
[16] T. D. Lee and C.-N. Yang, Phys. Rev. **108**, 1645 (1957).
[17] M. Ablikim *et al.* (BESIII Collaboration), Nat. Phys. **15**, 631 (2019).
[18] M. Ablikim *et al.* (BESIII Collaboration), Nature (London) **606**, 64 (2022).
[19] M. Ablikim *et al.* (BESIII Collaboration), Chin. Phys. C **46**, 074001 (2022).
[20] E. Perotti, G. Fäldt, A. Kupsc, S. Leupold, and J. J. Song, Phys. Rev. D **99**, 056008 (2019).
[21] M. Ablikim *et al.* (BESIII Collaboration), Nucl. Instrum. Methods Phys. Res., Sect. A **614**, 345 (2010).
[22] K.-X. Huang, Z.-J. Li, Z. Qian, J. Zhu, H.-Y. Li, Y.-M. Zhang, S.-S. Sun, and Z.-Y. You, Nucl. Sci. Tech. **33**, 142 (2022).
[23] R.-G. Ping, Chin. Phys. C **32**, 599 (2008).
[24] Z.-Y. Deng *et al.*, Chin. Phys. C **30**, 371 (2006).
[25] W. Li *et al.*, *Proceeding of CHEP* (2006), Vol. 27.
[26] S. Agostinelli *et al.* (GEANT4 Collaboration), Nucl. Instrum. Methods Phys. Res., Sect. A **506**, 250 (2003).
[27] J. R. Klein and A. Roodman, Annu. Rev. Nucl. Part. Sci. **55**, 141 (2005).
[28] M. Xu *et al.*, Chin. Phys. C **34**, 92 (2010).
[29] R. L. Workman and Others (Particle Data Group Collaboration), Prog. Theor. Exp. Phys. **2022**, 083C01 (2022).
[30] J. Therhaag, Proc. Sci. ICHEP2010 (**2010**) 510.
[31] The *deposited energy* is the total cluster energy of a shower denoted as $E_{\rm tot}$. The *hit number* is the total number of the ignited crystals of a shower denoted as $N_{\rm hit}$. The *secondary moment* is defined as $\sum_i (E_i r_i^2/E_{\rm tot})$. The *Zernike moment* ($A_{42}$) is defined as $|\sum_i (E_i/E_{\rm tot}) f_{4,2}(r_i/R_0) e^{im\phi_i}|$ with the coefficient $f_{4,2} = 4x^4 - 3x^2$, where r_i and ϕ_i are the radial and angular separation of crystal i with respect to the cluster center, E_i is the ith ignited crystals, and R_0 is a cutoff radius of 15 cm. The deposition shape is defined as $(E_{3\times3} - E_{\rm seed})/E_{3\times3}$ and $(E_{\rm tot} - E_{\rm seed})/[(N_{\rm hit} - 1) \times E_{\rm tot}]$, where $E_{3\times3}$ are the deposited energies in 3×3 crystals around the cluster seed.
[32] X. Zhou, S. Du, G. Li, and C. Shen, Comput. Phys. Commun. **258**, 107540 (2021).
[33] H. Albrecht *et al.* (ARGUS Collaboration), Phys. Lett. B **241**, 278 (1990).
[34] See Supplemental Material at http://link.aps.org/supplemental/10.1103/PhysRevLett.132.101801 for additional details on the study of systematic uncertainties.
[35] C. Langenbruch, Eur. Phys. J. C **82**, 393 (2022).
[36] M. Hatlo, F. James, P. Mato, L. Moneta, M. Winkler, and A. Zsenei, IEEE Trans. Nucl. Sci. **52**, 2818 (2005).
[37] M. Ablikim *et al.* (BESIII Collaboration), Phys. Rev. Lett. **129**, 131801 (2022).
[38] T. Holmstrom *et al.* (HyperCP Collaboration), Phys. Rev. Lett. **93**, 262001 (2004).
[39] J. Tandean and G. Valencia, Phys. Rev. D **67**, 056001 (2003).
[40] X.-G. He, J. Tandean, and G. Valencia, Sci. Bull. **67**, 1840 (2022).
[41] M. Hoferichter, J. Ruiz de Elvira, B. Kubis, and U.-G. Meißner, Phys. Rep. **625**, 1 (2016).

M. Ablikim,[1] M. N. Achasov,[5,b] P. Adlarson,[75] X. C. Ai,[81] R. Aliberti,[36] A. Amoroso,[74a,74c] M. R. An,[40] Q. An,[71,58] Y. Bai,[57] O. Bakina,[37] I. Balossino,[30a] Y. Ban,[47,g] V. Batozskaya,[1,45] K. Begzsuren,[33] N. Berger,[36] M. Berlowski,[45] M. Bertani,[29a] D. Bettoni,[30a] F. Bianchi,[74a,74c] E. Bianco,[74a,74c] A. Bortone,[74a,74c] I. Boyko,[37] R. A. Briere,[6] A. Brueggemann,[68] H. Cai,[76] X. Cai,[1,58] A. Calcaterra,[29a] G. F. Cao,[1,63] N. Cao,[1,63] S. A. Cetin,[62a] J. F. Chang,[1,58] T. T. Chang,[77] W. L. Chang,[1,63] G. R. Che,[44] G. Chelkov,[37,a] C. Chen,[44] Chao Chen,[55] G. Chen,[1] H. S. Chen,[1,63] M. L. Chen,[1,58,63] S. J. Chen,[43] S. L. Chen,[46] S. M. Chen,[61] T. Chen,[1,63] X. R. Chen,[32,63] X. T. Chen,[1,63] Y. B. Chen,[1,58] Y. Q. Chen,[35] Z. J. Chen,[26,h] W. S. Cheng,[74c] S. K. Choi,[11] X. Chu,[44] G. Cibinetto,[30a] S. C. Coen,[4] F. Cossio,[74c] J. J. Cui,[50] H. L. Dai,[1,58] J. P. Dai,[79] A. Dbeyssi,[19] R. E. de Boer,[4] D. Dedovich,[37] Z. Y. Deng,[1] A. Denig,[36] I. Denysenko,[37] M. Destefanis,[74a,74c] F. De Mori,[74a,74c] B. Ding,[66,1] X. X. Ding,[47,g] Y. Ding,[35] Y. Ding,[41] J. Dong,[1,58] L. Y. Dong,[1,63] M. Y. Dong,[1,58,63] X. Dong,[76] M. C. Du,[1] S. X. Du,[81] Z. H. Duan,[43] P. Egorov,[37,a] Y. H. Fan,[46] J. Fang,[1,58] S. S. Fang,[1,63] W. X. Fang,[1] Y. Fang,[1] R. Farinelli,[30a] L. Fava,[74b,74c] F. Feldbauer,[4] G. Felici,[29a] C. Q. Feng,[71,58] J. H. Feng,[59] K. Fischer,[69] M. Fritsch,[4] C. D. Fu,[1] J. L. Fu,[63] Y. W. Fu,[1] H. Gao,[63] Y. N. Gao,[47,g] Yang Gao,[71,58] S. Garbolino,[74c] I. Garzia,[30a,30b] P. T. Ge,[76] Z. W. Ge,[43] C. Geng,[59] E. M. Gersabeck,[67] A. Gilman,[69] K. Goetzen,[14] L. Gong,[41] W. X. Gong,[1,58] W. Gradl,[36] S. Gramigna,[30a,30b] M. Greco,[74a,74c] M. H. Gu,[1,58] Y. T. Gu,[16] C. Y. Guan,[1,63] Z. L. Guan,[23] A. Q. Guo,[32,63] L. B. Guo,[42] M. J. Guo,[50] R. P. Guo,[49] Y. P. Guo,[13,f] A. Guskov,[37,a] T. T. Han,[50] W. Y. Han,[40] X. Q. Hao,[20] F. A. Harris,[65] K. K. He,[55] K. L. He,[1,63] F. H. H. Heinsius,[4] C. H. Heinz,[36] Y. K. Heng,[1,58,63] C. Herold,[60] T. Holtmann,[4] P. C. Hong,[13,f] G. Y. Hou,[1,63] X. T. Hou,[1,63] Y. R. Hou,[63] Z. L. Hou,[1] H. M. Hu,[1,63] J. F. Hu,[56,i] T. Hu,[1,58,63] Y. Hu,[1] G. S. Huang,[71,58] K. X. Huang,[59] L. Q. Huang,[32,63] X. T. Huang,[50] Y. P. Huang,[1] T. Hussain,[73] N. Hüsken,[28,36] N. in der Wiesche,[68] M. Irshad,[71,58] J. Jackson,[28] S. Jaeger,[4] S. Janchiv,[33] J. H. Jeong,[11] Q. Ji,[1] Q. P. Ji,[20] X. B. Ji,[1,63] X. L. Ji,[1,58] Y. Y. Ji,[50] X. Q. Jia,[50] Z. K. Jia,[71,58] H. J. Jiang,[76] P. C. Jiang,[47,g] S. S. Jiang,[40] T. J. Jiang,[17] X. S. Jiang,[1,58,63] Y. Jiang,[63] J. B. Jiao,[50] Z. Jiao,[24] S. Jin,[43] Y. Jin,[66] M. Q. Jing,[1,63] T. Johansson,[75] X. K.,[1] S. Kabana,[34] N. Kalantar-Nayestanaki,[64] X. L. Kang,[10] X. S. Kang,[41] M. Kavatsyuk,[64] B. C. Ke,[81] A. Khoukaz,[68] R. Kiuchi,[1] R. Kliemt,[14] O. B. Kolcu,[62a] B. Kopf,[4] M. Kuessner,[4] A. Kupsc,[45,75] W. Kühn,[38] J. J. Lane,[67] P. Larin,[19] A. Lavania,[27] L. Lavezzi,[74a,74c] T. T. Lei,[71,58] Z. H. Lei,[71,58] H. Leithoff,[36] M. Lellmann,[36] T. Lenz,[36] C. Li,[44] C. Li,[48] C. H. Li,[40] Cheng Li,[71,58] D. M. Li,[81] F. Li,[1,58] G. Li,[1] H. Li,[71,58] H. B. Li,[1,63] H. J. Li,[20] H. N. Li,[56,i] Hui Li,[44] J. R. Li,[61] J. S. Li,[59] J. W. Li,[50] K. L. Li,[20] Ke Li,[1] L. J. Li,[1,63] L. K. Li,[1] Lei Li,[3] M. H. Li,[44] P. R. Li,[39,j,k] Q. X. Li,[50] S. X. Li,[13] T. Li,[50] W. D. Li,[1,63] W. G. Li,[1] X. H. Li,[71,58] X. L. Li,[50] Xiaoyu Li,[1,63] Y. G. Li,[47,g] Z. J. Li,[59] Z. X. Li,[16] C. Liang,[43] H. Liang,[1,63] H. Liang,[35] H. Liang,[71,58] Y. F. Liang,[54] Y. T. Liang,[32,63] G. R. Liao,[15] L. Z. Liao,[50] Y. P. Liao,[1,63] J. Libby,[27] A. Limphirat,[60] D. X. Lin,[32,63] T. Lin,[1] B. J. Liu,[1] B. X. Liu,[76] C. Liu,[35] C. X. Liu,[1] F. H. Liu,[53] Fang Liu,[1] Feng Liu,[7] G. M. Liu,[56,i] H. Liu,[39,j,k] H. B. Liu,[16] H. M. Liu,[1,63] Huanhuan Liu,[1] Huihui Liu,[22] J. B. Liu,[71,58] J. L. Liu,[72] J. Y. Liu,[1,63] K. Liu,[1] K. Y. Liu,[41] Ke Liu,[23] L. Liu,[71,58] L. C. Liu,[44] Lu Liu,[44] M. H. Liu,[13,f] P. L. Liu,[1] Q. Liu,[63] S. B. Liu,[71,58] T. Liu,[13,f] W. K. Liu,[44] W. M. Liu,[71,58] X. Liu,[39,j,k] Y. Liu,[39,j,k] Y. Liu,[81] Y. B. Liu,[44] Z. A. Liu,[1,58,63] Z. Q. Liu,[50] X. C. Lou,[1,58,63] F. X. Lu,[59] H. J. Lu,[24] J. G. Lu,[1,58] X. L. Lu,[1] Y. Lu,[8] Y. P. Lu,[1,58] Z. H. Lu,[1,63] C. L. Luo,[42] M. X. Luo,[80] T. Luo,[13,f] X. L. Luo,[1,58] X. R. Lyu,[63] Y. F. Lyu,[44] F. C. Ma,[41] H. L. Ma,[1] J. L. Ma,[1,63] L. L. Ma,[50] M. M. Ma,[1,63] Q. M. Ma,[1] R. Q. Ma,[1,63] R. T. Ma,[63] X. Y. Ma,[1,58] Y. Ma,[47,g] Y. M. Ma,[32] F. E. Maas,[19] M. Maggiora,[74a,74c] S. Malde,[69] Q. A. Malik,[73] A. Mangoni,[29b] Y. J. Mao,[47,g] Z. P. Mao,[1] S. Marcello,[74a,74c] Z. X. Meng,[66] J. G. Messchendorp,[14,64] G. Mezzadri,[30a] H. Miao,[1,63] T. J. Min,[43] R. E. Mitchell,[28] X. H. Mo,[1,58,63] N. Yu. Muchnoi,[5,b] J. Muskalla,[36] Y. Nefedov,[37] F. Nerling,[19,d] I. B. Nikolaev,[5,b] Z. Ning,[1,58] S. Nisar,[12,l] Q. L. Niu,[39,j,k] W. D. Niu,[55] Y. Niu,[50] S. L. Olsen,[63] Q. Ouyang,[1,58,63] S. Pacetti,[29b,29c] X. Pan,[55] Y. Pan,[57] A. Pathak,[35] P. Patteri,[29a] Y. P. Pei,[71,58] M. Pelizaeus,[4] H. P. Peng,[71,58] Y. Y. Peng,[39,j,k] K. Peters,[14,d] J. L. Ping,[42] R. G. Ping,[1,63] S. Plura,[36] V. Prasad,[34] F. Z. Qi,[1] H. Qi,[71,58] H. R. Qi,[61] M. Qi,[43] T. Y. Qi,[13,f] S. Qian,[1,58] W. B. Qian,[63] C. F. Qiao,[63] J. J. Qin,[72] L. Q. Qin,[15] X. P. Qin,[13,f] X. S. Qin,[50] Z. H. Qin,[1,58] J. F. Qiu,[1] S. Q. Qu,[61] C. F. Redmer,[36] K. J. Ren,[40] A. Rivetti,[74c] M. Rolo,[74c] G. Rong,[1,63] Ch. Rosner,[19] S. N. Ruan,[44] N. Salone,[45] A. Sarantsev,[37,c] Y. Schelhaas,[36] K. Schoenning,[75] M. Scodeggio,[30a,30b] K. Y. Shan,[13,f] W. Shan,[25] X. Y. Shan,[71,58] J. F. Shangguan,[55] L. G. Shao,[1,63] M. Shao,[71,58] C. P. Shen,[13,f] H. F. Shen,[1,63] W. H. Shen,[63] X. Y. Shen,[1,63] B. A. Shi,[63] H. C. Shi,[71,58] J. L. Shi,[13] J. Y. Shi,[1] Q. Q. Shi,[55] R. S. Shi,[1,63] X. Shi,[1,58] J. J. Song,[20] T. Z. Song,[59] W. M. Song,[35,1] Y. J. Song,[13] Y. X. Song,[47,g] S. Sosio,[74a,74c] S. Spataro,[74a,74c] F. Stieler,[36] Y. J. Su,[63] G. B. Sun,[76] G. X. Sun,[1] H. Sun,[63] H. K. Sun,[1] J. F. Sun,[20] K. Sun,[61] L. Sun,[76] S. S. Sun,[1,63] T. Sun,[1,63] W. Y. Sun,[35] Y. Sun,[10] Y. J. Sun,[71,58] Y. Z. Sun,[1] Z. T. Sun,[50] Y. X. Tan,[71,58] C. J. Tang,[54] G. Y. Tang,[1] J. Tang,[59] Y. A. Tang,[76] L. Y. Tao,[72] Q. T. Tao,[26,h] M. Tat,[69] J. X. Teng,[71,58] V. Thoren,[75] W. H. Tian,[59] W. H. Tian,[52] Y. Tian,[32,63] Z. F. Tian,[76] I. Uman,[62b] S. J. Wang,[50] B. Wang,[1] B. L. Wang,[63] Bo Wang,[71,58] C. W. Wang,[43] D. Y. Wang,[47,g] F. Wang,[72] H. J. Wang,[39,j,k] H. P. Wang,[1,63] J. P. Wang,[50] K. Wang,[1,58] L. L. Wang,[1] M. Wang,[50] Meng Wang,[1,63] S. Wang,[13,f] S. Wang,[39,j,k] T. Wang,[13,f] T. J. Wang,[44] W. Wang,[72] W. Wang,[59] W. P. Wang,[71,58] X. Wang,[47,g] X. F. Wang,[39,j,k] X. J. Wang,[40] X. L. Wang,[13,f] Y. Wang,[61] Y. D. Wang,[46] Y. F. Wang,[1,58,63] Y. H. Wang,[48] Y. N. Wang,[46] Y. Q. Wang,[1] Yaqian Wang,[18,1] Yi Wang,[61] Z. Wang,[1,58] Z. L. Wang,[72] Z. Y. Wang,[1,63] Ziyi Wang,[63] D. Wei,[70] D. H. Wei,[15] F. Weidner,[68] S. P. Wen,[1] C. W. Wenzel,[4] U. Wiedner,[4] G. Wilkinson,[69] M. Wolke,[75] L. Wollenberg,[4] C. Wu,[40] J. F. Wu,[1,63] L. H. Wu,[1] L. J. Wu,[1,63] X. Wu,[13,f] X. H. Wu,[35] Y. Wu,[71] Y. H. Wu,[55] Y. J. Wu,[32] Z. Wu,[1,58] L. Xia,[71,58] X. M. Xian,[40] T. Xiang,[47,g] D. Xiao,[39,j,k] G. Y. Xiao,[43] S. Y. Xiao,[1] Y. L. Xiao,[13,f] Z. J. Xiao,[42] C. Xie,[43] X. H. Xie,[47,g] Y. Xie,[50] Y. G. Xie,[1,58] Y. H. Xie,[7] Z. P. Xie,[71,58] T. Y. Xing,[1,63] C. F. Xu,[1,63] C. J. Xu,[59] G. F. Xu,[1] H. Y. Xu,[66] Q. J. Xu,[17] Q. N. Xu,[31] W. Xu,[1,63] W. L. Xu,[66] X. P. Xu,[55] Y. C. Xu,[78] Z. P. Xu,[43] Z. S. Xu,[63] F. Yan,[13,f] L. Yan,[13,f] W. B. Yan,[71,58] W. C. Yan,[81] X. Q. Yan,[1] H. J. Yang,[51,e] H. L. Yang,[35] H. X. Yang,[1] Tao Yang,[1] Y. Yang,[13,f] Y. F. Yang,[44] Y. X. Yang,[1,63] Yifan Yang,[1,63] Z. W. Yang,[39,j,k] Z. P. Yao,[50] M. Ye,[1,58] M. H. Ye,[9] J. H. Yin,[1] Z. Y. You,[59] B. X. Yu,[1,58,63] C. X. Yu,[44] G. Yu,[1,63] J. S. Yu,[26,h] T. Yu,[72] X. D. Yu,[47,g] C. Z. Yuan,[1,63] L. Yuan,[2] S. C. Yuan,[1] X. Q. Yuan,[1] Y. Yuan,[1,63] Z. Y. Yuan,[59] C. X. Yue,[40] A. A. Zafar,[73] F. R. Zeng,[50] X. Zeng,[13,f] Y. Zeng,[26,h] Y. J. Zeng,[1,63] X. Y. Zhai,[35] Y. C. Zhai,[50] Y. H. Zhan,[59] A. Q. Zhang,[1,63] B. L. Zhang,[1,63] B. X. Zhang,[1] D. H. Zhang,[44] G. Y. Zhang,[20] H. Zhang,[71] H. C. Zhang,[1,58,63] H. H. Zhang,[59] H. H. Zhang,[35] H. Q. Zhang,[1,58,63] H. Y. Zhang,[1,58] J. Zhang,[81] J. J. Zhang,[52] J. L. Zhang,[21] J. Q. Zhang,[42] J. W. Zhang,[1,58,63] J. X. Zhang,[39,j,k] J. Y. Zhang,[1] J. Z. Zhang,[1,63] Jianyu Zhang,[63] Jiawei Zhang,[1,63] L. M. Zhang,[61] L. Q. Zhang,[59] Lei Zhang,[43] P. Zhang,[1,63] Q. Y. Zhang,[40,81] Shuihan Zhang,[1,63] Shulei Zhang,[26,h] X. D. Zhang,[46] X. M. Zhang,[1] X. Y. Zhang,[50] Xuyan Zhang,[55] Y. Zhang,[69] Y. Zhang,[72] Y. T. Zhang,[81] Y. H. Zhang,[1,58] Yan Zhang,[71,58] Yao Zhang,[1] Z. H. Zhang,[1] Z. L. Zhang,[35] Z. Y. Zhang,[44] Z. Y. Zhang,[76] G. Zhao,[1] J. Zhao,[40] J. Y. Zhao,[1,63] J. Z. Zhao,[1,58] Lei Zhao,[71,58] Ling Zhao,[1] M. G. Zhao,[44] S. J. Zhao,[81] Y. B. Zhao,[1,58] Y. X. Zhao,[32,63] Z. G. Zhao,[71,58] A. Zhemchugov,[37,a] B. Zheng,[72] J. P. Zheng,[1,58] W. J. Zheng,[1,63] Y. H. Zheng,[63] B. Zhong,[42] X. Zhong,[59] H. Zhou,[50] L. P. Zhou,[1,63] X. Zhou,[76] X. K. Zhou,[7] X. R. Zhou,[71,58] X. Y. Zhou,[40] Y. Z. Zhou,[13,f] J. Zhu,[44] K. Zhu,[1] K. J. Zhu,[1,58,63] L. Zhu,[35] L. X. Zhu,[63] S. H. Zhu,[70] S. Q. Zhu,[43] T. J. Zhu,[13,f] W. J. Zhu,[13,f] Y. C. Zhu,[71,58] Z. A. Zhu,[1,63] J. H. Zou,[1] and J. Zu[71,58]

(BESIII Collaboration)

[1]*Institute of High Energy Physics, Beijing 100049, People's Republic of China*
[2]*Beihang University, Beijing 100191, People's Republic of China*
[3]*Beijing Institute of Petrochemical Technology, Beijing 102617, People's Republic of China*
[4]*Bochum Ruhr-University, D-44780 Bochum, Germany*
[5]*Budker Institute of Nuclear Physics SB RAS (BINP), Novosibirsk 630090, Russia*
[6]*Carnegie Mellon University, Pittsburgh, Pennsylvania 15213, USA*
[7]*Central China Normal University, Wuhan 430079, People's Republic of China*
[8]*Central South University, Changsha 410083, People's Republic of China*
[9]*China Center of Advanced Science and Technology, Beijing 100190, People's Republic of China*
[10]*China University of Geosciences, Wuhan 430074, People's Republic of China*
[11]*Chung-Ang University, Seoul, 06974, Republic of Korea*
[12]*COMSATS University Islamabad, Lahore Campus, Defence Road, Off Raiwind Road, 54000 Lahore, Pakistan*
[13]*Fudan University, Shanghai 200433, People's Republic of China*
[14]*GSI Helmholtzcentre for Heavy Ion Research GmbH, D-64291 Darmstadt, Germany*
[15]*Guangxi Normal University, Guilin 541004, People's Republic of China*
[16]*Guangxi University, Nanning 530004, People's Republic of China*
[17]*Hangzhou Normal University, Hangzhou 310036, People's Republic of China*
[18]*Hebei University, Baoding 071002, People's Republic of China*
[19]*Helmholtz Institute Mainz, Staudinger Weg 18, D-55099 Mainz, Germany*
[20]*Henan Normal University, Xinxiang 453007, People's Republic of China*
[21]*Henan University, Kaifeng 475004, People's Republic of China*
[22]*Henan University of Science and Technology, Luoyang 471003, People's Republic of China*
[23]*Henan University of Technology, Zhengzhou 450001, People's Republic of China*
[24]*Huangshan College, Huangshan 245000, People's Republic of China*
[25]*Hunan Normal University, Changsha 410081, People's Republic of China*
[26]*Hunan University, Changsha 410082, People's Republic of China*
[27]*Indian Institute of Technology Madras, Chennai 600036, India*
[28]*Indiana University, Bloomington, Indiana 47405, USA*
[29a]*INFN Laboratori Nazionali di Frascati, INFN Laboratori Nazionali di Frascati, I-00044, Frascati, Italy*

[29b]INFN Sezione di Perugia, I-06100, Perugia, Italy
[29c]University of Perugia, I-06100, Perugia, Italy
[30a]INFN Sezione di Ferrara, INFN Sezione di Ferrara, I-44122, Ferrara, Italy
[30b]University of Ferrara, I-44122, Ferrara, Italy
[31]Inner Mongolia University, Hohhot 010021, People's Republic of China
[32]Institute of Modern Physics, Lanzhou 730000, People's Republic of China
[33]Institute of Physics and Technology, Peace Avenue 54B, Ulaanbaatar 13330, Mongolia
[34]Instituto de Alta Investigación, Universidad de Tarapacá, Casilla 7D, Arica 1000000, Chile
[35]Jilin University, Changchun 130012, People's Republic of China
[36]Johannes Gutenberg University of Mainz, Johann-Joachim-Becher-Weg 45, D-55099 Mainz, Germany
[37]Joint Institute for Nuclear Research, 141980 Dubna, Moscow region, Russia
[38]Justus-Liebig-Universitaet Giessen, II. Physikalisches Institut, Heinrich-Buff-Ring 16, D-35392 Giessen, Germany
[39]Lanzhou University, Lanzhou 730000, People's Republic of China
[40]Liaoning Normal University, Dalian 116029, People's Republic of China
[41]Liaoning University, Shenyang 110036, People's Republic of China
[42]Nanjing Normal University, Nanjing 210023, People's Republic of China
[43]Nanjing University, Nanjing 210093, People's Republic of China
[44]Nankai University, Tianjin 300071, People's Republic of China
[45]National Centre for Nuclear Research, Warsaw 02-093, Poland
[46]North China Electric Power University, Beijing 102206, People's Republic of China
[47]Peking University, Beijing 100871, People's Republic of China
[48]Qufu Normal University, Qufu 273165, People's Republic of China
[49]Shandong Normal University, Jinan 250014, People's Republic of China
[50]Shandong University, Jinan 250100, People's Republic of China
[51]Shanghai Jiao Tong University, Shanghai 200240, People's Republic of China
[52]Shanxi Normal University, Linfen 041004, People's Republic of China
[53]Shanxi University, Taiyuan 030006, People's Republic of China
[54]Sichuan University, Chengdu 610064, People's Republic of China
[55]Soochow University, Suzhou 215006, People's Republic of China
[56]South China Normal University, Guangzhou 510006, People's Republic of China
[57]Southeast University, Nanjing 211100, People's Republic of China
[58]State Key Laboratory of Particle Detection and Electronics, Beijing 100049, Hefei 230026, People's Republic of China
[59]Sun Yat-Sen University, Guangzhou 510275, People's Republic of China
[60]Suranaree University of Technology, University Avenue 111, Nakhon Ratchasima 30000, Thailand
[61]Tsinghua University, Beijing 100084, People's Republic of China
[62a]Turkish Accelerator Center Particle Factory Group, Istinye University, 34010, Istanbul, Turkey
[62b]Near East University, Nicosia, North Cyprus, 99138, Mersin 10, Turkey
[63]University of Chinese Academy of Sciences, Beijing 100049, People's Republic of China
[64]University of Groningen, NL-9747 AA Groningen, The Netherlands
[65]University of Hawaii, Honolulu, Hawaii 96822, USA
[66]University of Jinan, Jinan 250022, People's Republic of China
[67]University of Manchester, Oxford Road, Manchester, M13 9PL, United Kingdom
[68]University of Muenster, Wilhelm-Klemm-Strasse 9, 48149 Muenster, Germany
[69]University of Oxford, Keble Road, Oxford OX13RH, United Kingdom
[70]University of Science and Technology Liaoning, Anshan 114051, People's Republic of China
[71]University of Science and Technology of China, Hefei 230026, People's Republic of China
[72]University of South China, Hengyang 421001, People's Republic of China
[73]University of the Punjab, Lahore-54590, Pakistan
[74a]University of Turin and INFN, University of Turin, I-10125, Turin, Italy
[74b]University of Eastern Piedmont, I-15121, Alessandria, Italy
[74c]INFN, I-10125, Turin, Italy
[75]Uppsala University, Box 516, SE-75120 Uppsala, Sweden
[76]Wuhan University, Wuhan 430072, People's Republic of China
[77]Xinyang Normal University, Xinyang 464000, People's Republic of China
[78]Yantai University, Yantai 264005, People's Republic of China
[79]Yunnan University, Kunming 650500, People's Republic of China
[80]Zhejiang University, Hangzhou 310027, People's Republic of China
[81]Zhengzhou University, Zhengzhou 450001, People's Republic of China

[a]Also at the Moscow Institute of Physics and Technology, Moscow 141700, Russia.
[b]Also at the Novosibirsk State University, Novosibirsk, 630090, Russia.
[c]Also at the NRC "Kurchatov Institute", PNPI, 188300, Gatchina, Russia.
[d]Also at Goethe University Frankfurt, 60323 Frankfurt am Main, Germany.
[e]Also at Key Laboratory for Particle Physics, Astrophysics and Cosmology, Ministry of Education; Shanghai Key Laboratory for Particle Physics and Cosmology; Institute of Nuclear and Particle Physics, Shanghai 200240, People's Republic of China.
[f]Also at Key Laboratory of Nuclear Physics and Ion-beam Application (MOE) and Institute of Modern Physics, Fudan University, Shanghai 200443, People's Republic of China.
[g]Also at State Key Laboratory of Nuclear Physics and Technology, Peking University, Beijing 100871, People's Republic of China.
[h]Also at School of Physics and Electronics, Hunan University, Changsha 410082, China.
[i]Also at Guangdong Provincial Key Laboratory of Nuclear Science, Institute of Quantum Matter, South China Normal University, Guangzhou 510006, China.
[j]Also at Frontiers Science Center for Rare Isotopes, Lanzhou University, Lanzhou 730000, People's Republic of China.
[k]Also at Lanzhou Center for Theoretical Physics, Lanzhou University, Lanzhou 730000, People's Republic of China.
[l]Also at the Department of Mathematical Sciences, IBA, Karachi 75270, Pakistan.